

# Numerical simulation of cutting capacity of shaped charge in blasting demolition of steel construction

Kaida Dai\*<sup>†</sup>, Masatoshi Kato\*\*<sup>\*</sup>, Kunihisa Katsuyama\*<sup>\*</sup>, Chul-Gi Suk\*\*\*<sup>\*</sup>,  
Jun Yang\*\*\*\*<sup>\*</sup>, and Pengwan Chen\*\*\*\*<sup>\*</sup>

\*Dept. Rural Engineering, Faculty of Agriculture, Ehime University, Matsuyama 790-8566, JAPAN

<sup>†</sup>Corresponding address: daikaida@agr.ehime-u.ac.jp

\*\*Architecture and Design Division, Penta-Ocean Construction Co., Ltd., 2-2-8 Kouraku, Bunkyo, Tokyo 112-8576, JAPAN

\*\*\*Korea Kacoh Co., Ltd., Seoul, KOREA

\*\*\*\*State Key Laboratory of Explosion Science and Technology, Beijing 100081, CHINA

Received : April 27, 2007 Accepted : November 15, 2007

## Abstract

This paper presents numerical simulation of the formation, the fragmentation, and the penetration into plates of metal jets that develops in a linear shaped charge. A fluid-structure coupling algorithm and an Arbitrary Lagrangian- Eulerian (ALE) method were used to treat the large deformation of the metal jet. The cutting results of simulation are compared with the test data, an agreement is reasonably good. The larger density of the liner material is noticeable to improve the cutting capability. The effect of standoff distance and the ultimate strength of steel plates were also considered. The simulation demonstrates the importance of the standoff distance and shows that the cutting depths decrease with the increasing of ultimate strength of steel plates.

**Keywords:** Numerical simulation, Shaped charges, Blasting demolition, Fluid-structure coupling.

## 1. Introduction

In the engineering blasting field, we must cut the complex steel structures in order to perform explosive demolition of the Steel Framed Reinforced Concrete (SRC). The steel pile can not be destroyed by general explosives. To control demolition effect, LSC (linear shaped charge) is used to cut complex steel structures with a continuous, high velocity, planar jet. The original theory of shaped charges was proposed by Brikhoff et al<sup>1)</sup>. More detail theories and the computational treatment of shaped charges can be found in the book by Walters and Zukas<sup>2)</sup>. Many experimental and computational studies have investigated the formation of metal jet and the influence factors of jet penetration into target. These factors include (1) liner angle; (2) shape factors; (3) liner material; (4) explosive and (5) standoff distance. A relation of penetration and standoff of shaped charge was reported by Eichelberger<sup>3)</sup>, from which one notes that from 5 up to 7 charge diameters, the penetration in a RHA (Rolled Homogenous

Armor) target is maximum. The experimental work by Trishin<sup>4)</sup> was showed that steel jets break into separate fragments while copper jets continue to stretch at the same times without visible rupture, the depth of penetration into targets is always smaller for steel jets than for copper jets. George<sup>5)</sup> demonstrated that material properties and LSC liner geometry play an important role in determining the size, shape and velocity of LSC fragments, and influence the collapse mechanism.

Experimental investigation is a main method in studying the impact fracture mechanisms of steel plates with LSC, being the development of high speed computers and powerful codes that give researchers to modeling experiment. Gazonas et al<sup>6)</sup> used Lagrangian hydrocode EPIC92 to simulate the formation of jet from a linear shaped charge and penetration into an RHA plate. Murphy et al<sup>7)</sup> have modeled the jet penetration process with CALE, a two dimensional arbitrary Lagrange Eulerian hydrocode.

The action of LSC includes: explosive detonation, liner

collapse, metal jet formation and stretch, cutting steel structure. The large deformation of conical liner needs use of hydrocode. This paper presents numerical analysis of the LSC cutting the steel plates. The cutting depth is compared with the experimental data. Besides the standoff distance, the influence of the liner material and the ultimate strength of steel plates are also considered. The analysis demonstrates the importance of standoff distance, liner material and the ultimate strength of steel plate.

### 2. Experiment of LSC

Figure 1 shows that the explosion phenomenon and the jet motion (white lines) of linear shaped charge. The explosive was ignited by a precise detonator of Nippon Kayaku Co.ltd at the end of the shaped charge. The photographs were observed using a high speed framing camera (Cordin model 124). This camera can take 26 pictures at a framing rate of  $1.0 \times 10^5 - 2.5 \times 10^6$  frames per second (FPS). In this experiment, a framing rate of  $5 \times 10^5$  was used and the interframe time was 2  $\mu$ sec. The results of experiment show that the detonation wave travels through the charge, and the focusing of the explosive high pressure causes the metal liner to collapse and form the cutting jet. The jet moves parallel and synchronous due to the short time of detonation propagation. Figure 2 shows that the cutting phenomenon of LSC. The cutting process is carried out from 6  $\mu$ sec to 8  $\mu$ sec, and by 8  $\mu$ sec, the target is completely cut by jet. It indicates that the crack of target is opened at the same time (frame 2 in Fig. 2), which can be related to the fact that the jet of whole LSC contacts

the target synchronously. The 2-dimensional model was used to investigate the cutting capacity of LSC according to the above-mentioned cutting concept. The cross section of LSC is illustrated in Fig. 3. LSC consists of the liner, outer case and explosive. Copper and steel were chosen as materials of the liner. The thickness of liner is 0.8 mm and the liner angle is 90 degree. The outer case was made of hard vinyl chloride. The high explosive was Pentolite. The length of LSC varied from 330 mm to 370 mm; other geometrical parameters of LSC were seen in Table 1. The effect of different standoff distance and steel plate material were considered.

### 3. Simulation of LSC

The 2D finite element model is generated with the pre-processor ANSYS. A part of LSC is modeled by adding z-coordinate constraint. The air is used for the region near the shaped charge and the path of jet. By making of symmetry, only 1/2 of the structure is modeled, shown in Fig. 4. The liner and explosive material are filled into the Eulerian grid where regular cubic brick elements are generated for all the parts. Fine meshes are generated for the steel target near air, the element size is  $0.2 \times 0.2$  (mm). Coarse meshes are applied for the remaining steel target so as to reduce the total number of element. These meshes are modeled as Lagrangian mesh. The mesh of model is shown in Fig. 5 and Fig. 6. To form the symmetry condition in the finite element model, the transitional displacement normal to symmetry planes is constrained.

The explosive has been modeled using a JWL equation

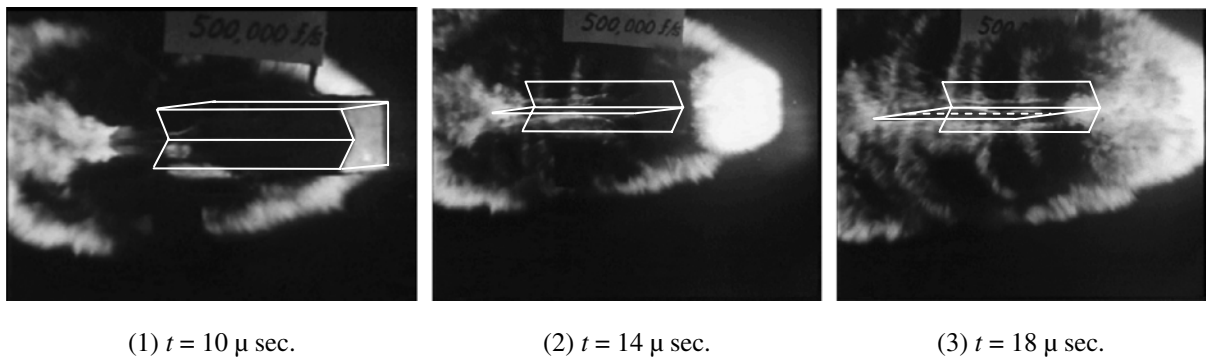


Fig. 1 The explosion phenomenon and jet motion. ( $t$ : time from initiation)

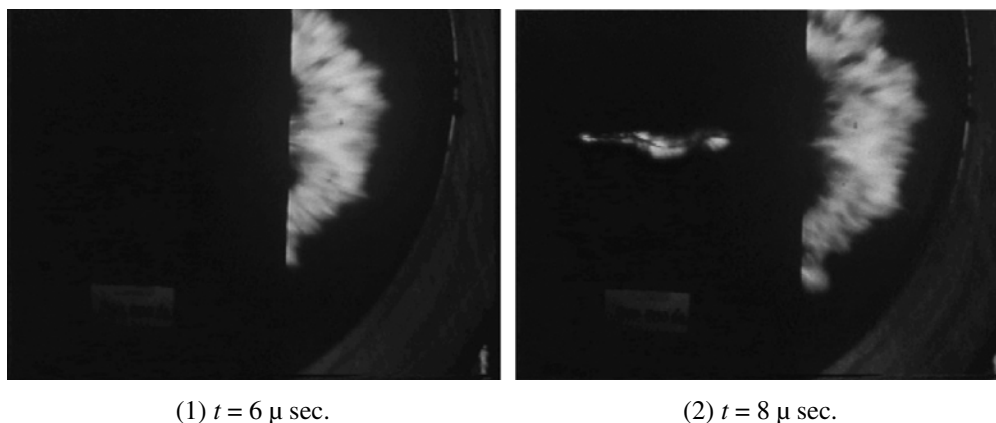


Fig. 2 The cutting phenomenon. ( $t$ : time from initiation)

Table 1 The model parameters of linear shaped charge.

N	Metal liner	Steel plate	$t$ (mm)	$T$ (mm)	$H$ (mm)	$W$ (mm)	$S$ (mm)	$D$ (mm)						
1		SS400	19				5	16.2						
							10	19.1						
							15	20.6						
							20	22.6						
2	Copper	SS400	28		15	20	25	24.8						
							30	23.6						
							35	22.4						
							40	20.2						
							3	SS400					8	13.4
4	SM490A					8	12.8							
5	SA440B	19		12	16	8	11.4							
6	HITEN690B					8	10.6							
7	HITEN780B					8	9.8							
8		SS400	19	3			5	15.4						
							10	18.2						
							15	20.4						
							20	22.0						
							25	23.4						
9	Steel	SS400	28		15	20	30	22.6						
							35	21.6						
							40	20.0						
							10	SS400					8	12.4
							11	SM490A					8	11.6
12	SA440B	19		12	16	8	10.2							
13	HITEN690B					8	9.4							
14	HITEN780B					8	9.0							

$t$ : Thickness of steel plate,  $T$ : Thickness of case,  $H$ : Height of explosive.

$W$ : Width of explosive,  $S$ : Standoff distance,  $D$ : Depth of cutting.

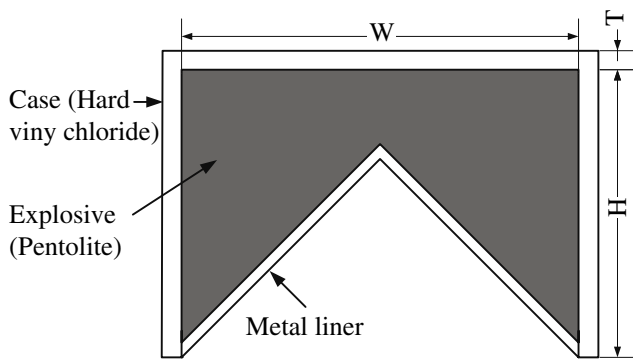


Fig. 3 The configuration of LSC.

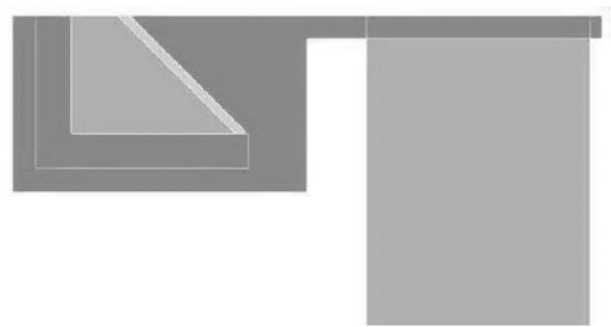


Fig. 4 Geometry of the model.

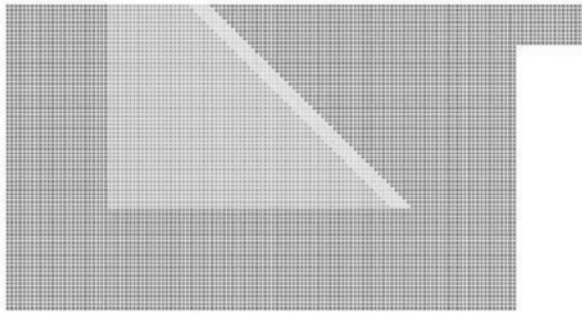


Fig. 5 Eulerian meshes for explosive, liner and air.

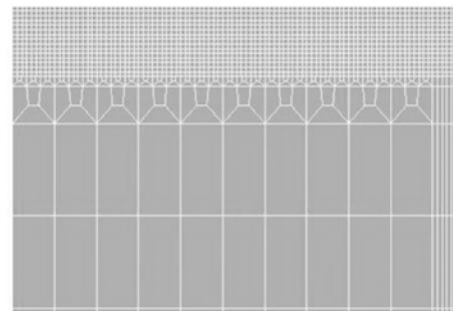


Fig. 6 Steel mesh.

Table 2 Parameters of PETN explosive.

Density (g • cm <sup>-3</sup> )	Detonation velocity (m • s <sup>-1</sup> )	CJ pressure (Gpa)	A (Gpa)	B (Gpa)	R <sub>1</sub>	R <sub>2</sub>	ω	E (Gpa)
1.61	7,800	25	880	20	5.47	1.46	0.35	9.8

Table 3 Parameters of liner.

Material	Density (g • cm <sup>-3</sup> )	Shear Modulus (Gpa)	Yield Stress (Gpa)	C (m • s <sup>-1</sup> )	S <sub>1</sub>	S <sub>2</sub>	r <sub>0</sub>	α
Copper	8.93	47.7	0.12	3,940	1.49	0.0	2.02	0.47
Steel	7.84	80.0	0.19	4,570	1.49	0.0	1.93	0.0

Table 4 Mechanical properties of steel materials.

Material	σ <sub>y</sub> (Mpa)	σ <sub>u</sub> (Mpa)	YR (%)	EL (%)	HRB
Steel Plate (SS400)	262	429	61.0	33	94
Steel Plate (SM490A)	342	515	66.5	29	102
Steel Plate (SA440B)	468	639	73.2	19	110
Steel Plate (HITEN690B)	713	758	94.1	17	112
Steel Plate (HITEN780B)	854	892	95.7	15	115

σ<sub>y</sub>: Yield point, σ<sub>u</sub>: Ultimate strength, YR: Yield ratio, EL: Elongation, HRB: Rockwell hardness (Scale B)

of state. Values of PETN were calculated by using one of RIO-DB database which is established by Dr. Katsumi Tanaka, AIST<sup>8)</sup>. The material parameters are listed in Table 2. The Steinberg material<sup>9)</sup> and Grüneisen equation of state are used for liner; the data are shown in Table 3. Elasto-plastic type steel is modeled, failure is initially assumed to occur if  $\epsilon_{eff}^p > \epsilon_{max}^p$ , where  $\epsilon_{eff}^p$  is the effective plastic strain,  $\epsilon_{max}^p$  is failure strain for eroding element, the material data of different steel plates are obtained from reference<sup>10)</sup>, shown in Table 4.

#### 4. Results and discussions

##### 4.1 Comparison of simulation results of copper and steel liners

Figure 7 (a) and (b) shows that the density distribution during jet formation for LSC with two different material

liner. After the initiation of explosive, the liner is accelerated and collapsed under the high pressure by focusing of explosive's energy. The resulting collapsed forms jet and slug (4 μsec), and then because the tip is traveling faster than the rear, the jet and slug stretch, becoming longer. After a time elapse of 11 μsec from initiation, the jet is broken up into fragment. Thereafter, numerous fragments of jet and the first fragment of slug appear at 17 μsec. However, there are more fragments in the steel liner than that in the copper liner. It should result in a noticeable decrease in cutting depth.

Figure 8 (a) and (b) show cutting results of simulation 1 and 8 at the same standoff distances (5 mm). In general, for the process of shaped charge cutting steel, the main part of steel is cut by jet and the residual part is decoupled by slug<sup>11), 12)</sup>. However, in the present simulation, the jet

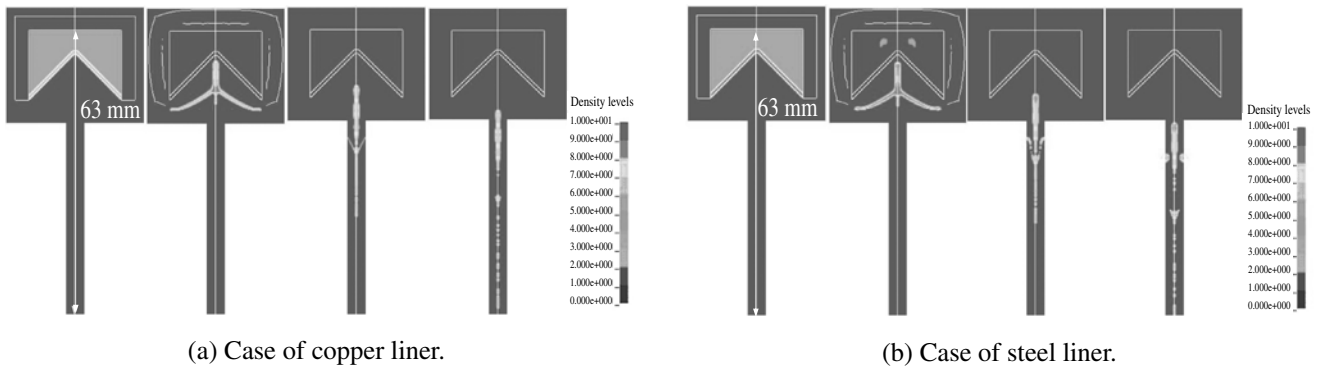


Fig. 7 Jet formation at four moments of time (0, 4, 11, 17  $\mu$  sec).

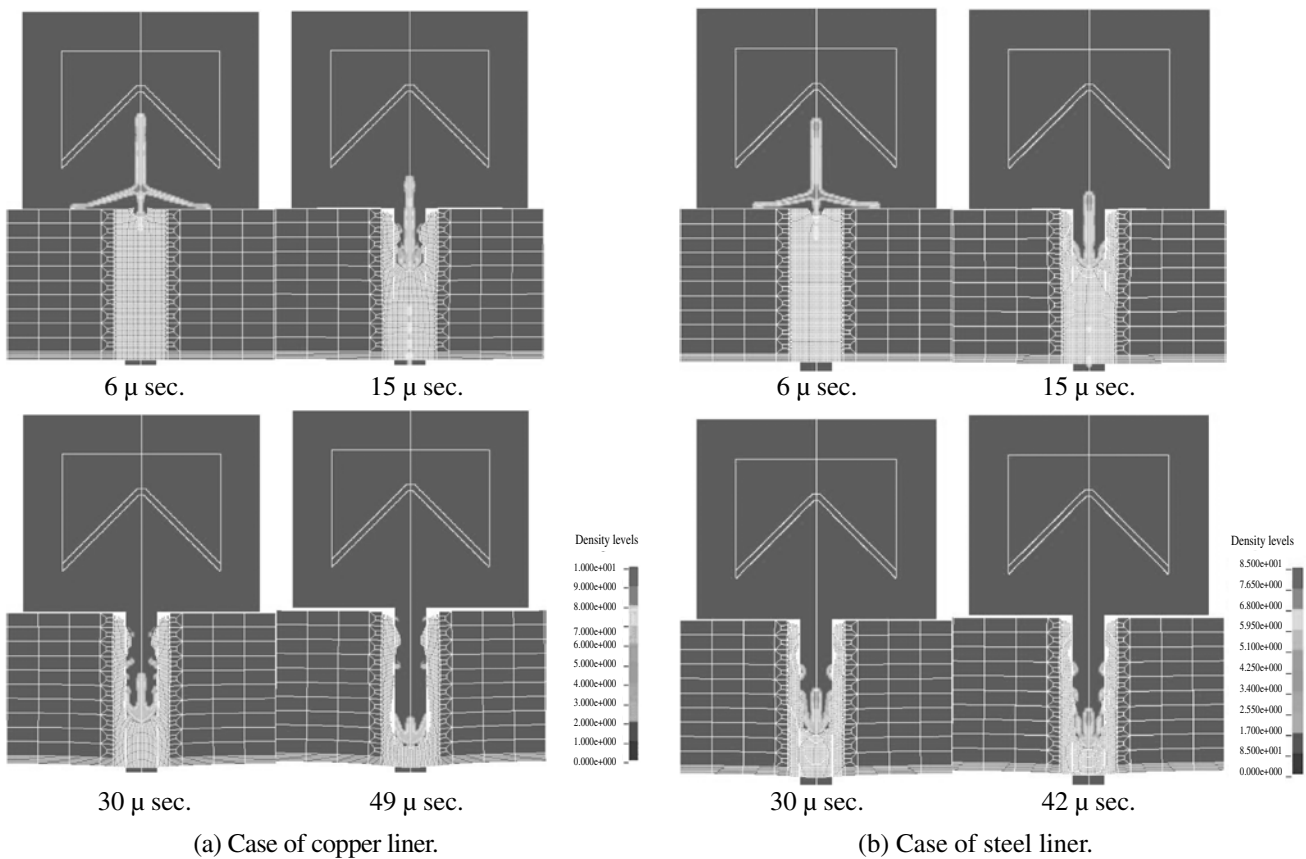


Fig. 8 The cutting results of simulation.

is not stretching because of the small stand off distance, so the steel is only cut by slug, which is noticeable in Fig. 8 (a) and (b). The slug hits the steel plate forcing it aside; the slug is used up and coats the inside of the hole as it cuts steel plate, the slug is gradually used up as it cuts the steel plate, and then the cutting process stops while the whole slug has been used up. Table 5 shows the cutting effect of different liners. The discrepancies between the computational and average experimental values are 16.8 % and 6.5 % respectively for simulation 1 and 8. The simulation result shows that cutting depth in the case of copper liner is bigger than that in the case of steel liner. This correlation is also confirmed in the case of 8 mm standoff distance as shown in Fig. 10. However the experimental results of 5 mm standoff distance which is summarized in Table 5 show the opposite tendency.

#### 4.2 Cutting depth of different standoff distance

Figure 9 (a) and (b) show the curve of cutting depth and standoff for simulation 2 and 9. It is observed that the decrease of the cutting depth occurs at a standoff distance of around 25 mm which represents 1.25 charge widths (the initial charge width is 20 mm). The simulation is agreement in theory and experimental work by Zhu Feng-chun who obtained that the optimal standoff is 1 charge widths<sup>13)</sup>. This can be related to the stretching, fragment of jet and slug.

#### 4.3 Cutting depth of different strength steel plate

Figure 10 (a) and (b) show the comparison of cutting depth of different ultimate strength steel plates at 8 mm standoff distances. The results show that the cutting depth decreases with the increasing of material ultimate strength

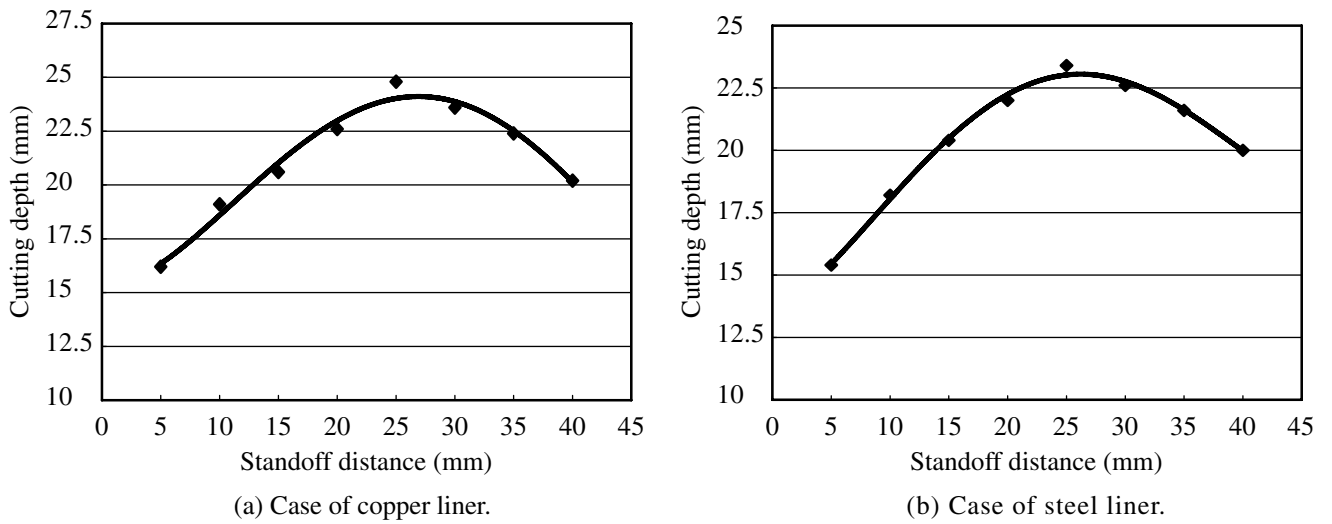
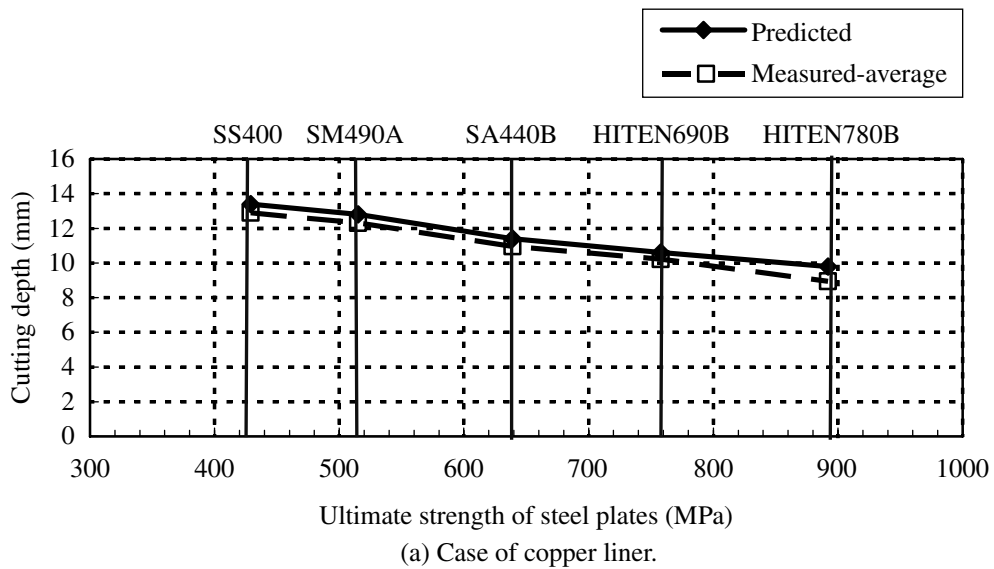
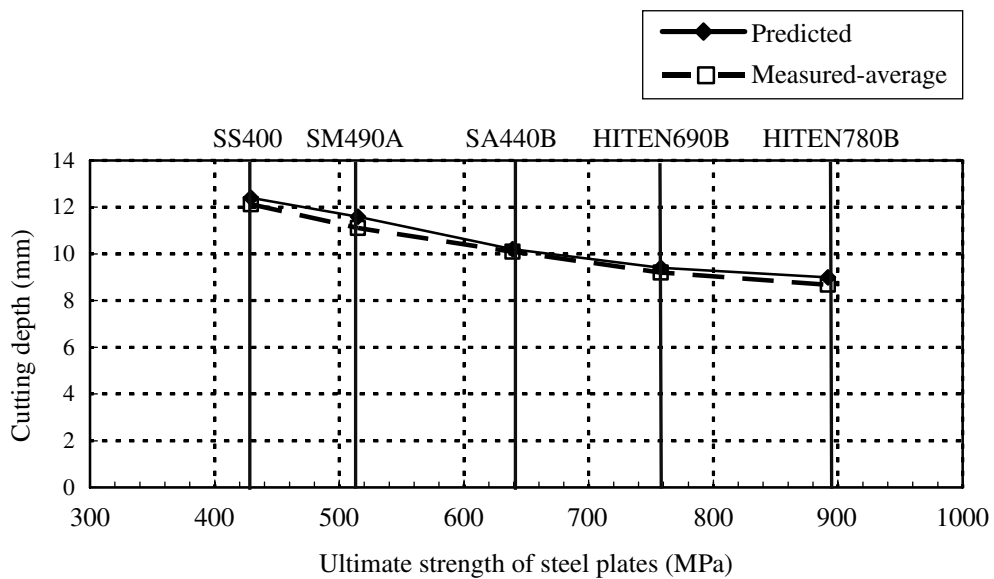


Fig. 9 The relation of cutting depth and standoff distance.



(a) Case of copper liner.



(b) Case of steel liner.

Fig. 10 Cutting depth vs ultimate strength of steel plates.

Table 5 Comparison of computational value and experimental value.

Liner	Cutting depth (mm)		
	Computational value	Experimental value	
		Maximum	Minimum
Copper	16.2	16.0	11.3
Steel	15.4	18.7	14.0

of steel plates. Agreement between the prediction and the experiment is achieved. The predicted values are slightly higher because the code is calculating performance of a perfect jet. The other reason of this behavior may be related to the dynamic properties of steel target which is significantly difficult to assume. Furthermore, the difficulties related on numerical technique still exist.

## 5. Conclusions

The jet formation and cutting effect of LSC presented this paper is based on ALE simulation method. The simulation results are agreement with experimental results. The numerical results show that different standoff distance result in different cutting depths, for LSC, the optimal standoff is 1.25 charge widths. The simulation also demonstrates that the liner material is an important factor affecting the resulting cutting depth achieved in the steel target. The larger density of the liner material is noticeable to improve the cutting capability. In addition, the simulation results show that the cutting depths decrease with the increasing of ultimate strength of steel plates, the material strength of steel plates is very important factor for cutting capacities of steel plates.

The 2D simulation gives us the cutting depth and the jet formation of a vertical section, but the understanding of the propagation of detonation wave and the whole jet profile is very difficult, so the 3D simulation should be executed to achieve the best effects.

## Acknowledgements

The authors would like to acknowledge Beijing Institute of Technology for the software support and thank Dr. Katsumi Tanaka who provided his assistance. Thanks for scholarship of the Foundation for the Industrial Explosives Technology.

## References

- 1) G. Birkhoff, D. MacDougall, E. Pugh and G. Taylor, *Journal of Applied Physics*, 19, 563 (1948).
- 2) W. P. Walters and J. A. Zukas, "Fundamentals of shaped charges" (1989), John Wiley and Sons.
- 3) R. J. Eichelberger, 11th Proceeding of the international symposium on ballistics, p. 379 (1989).
- 4) Y. A. Trishin, *Journal of Applied Mechanics and Technical Physics*, 41, 577 (2000).
- 5) G. A. Hayes, *Journal of materials science*, 19, 3049 (1984).
- 6) G. A. Gazonas, S. B. Segleters, S. R. Stegall and C. V. Paxton, AD-A299777 (1995).
- 7) M. J. Murphy, D. W. Baum, D. B. Clark, E. M. Mcguire and S. C. Simonson, 6th international conference on mechanical and physical behavior of materials under dynamic loading (2000), Krakow, Poland, September 25-29.
- 8) <http://riodb.ibase.aist.go.jp/ChemTherm/KHT3000>.
- 9) J. O. Hallquist, "LS-DYNA Keyword User's Manual", Version 970, April (2003), Livermore Software and Technology Corporation, Livermore CA.
- 10) M. Kato, Y. Nakamura, A. Matsuo, Y. Ogata, K. Katsuyama and K. hashizume, *Kayaku Gakkaishi (Sci. Tech. Energetic Materials)*, 61, 281 (2000).
- 11) H. Miyoshi, H. Ohba, H. Kitamura, T. Noue and T. Hiroe, *Sci. Tech. Energetic Materials*, 66, 340 (2005).
- 12) J. Bolstad and D. Mandell, LA-12274 (1992).
- 13) Zhu Fengchun, Deng Zhenli, Hu yu, *Initiators & Pyrotechnics*, 3, 20 (2000).